TOPICAL REVIEW — 2D materials: physics and device applications

Recent progress on integrating two-dimensional materials with ferroelectrics for memory devices and photodetectors*

Jianlu Wang(王建禄)† and Weida Hu(胡伟达)‡

National Laboratory for Infrared Physics, Shanghai Institute of Technical Physics, Chinese Academy of Sciences, Shanghai 200083, *China*

(Received 7 October 2016; revised manuscript received 24 November 2016; published online 13 February 2017)

Two-dimensional (2D) materials, such as graphene and MoS_2 related transition metal dichalcogenides (TMDC), have attracted much attention for their potential applications. Ferroelectrics, one of the special and traditional dielectric materials, possess a spontaneous electric polarization that can be reversed by the application of an external electric field. In recent years, a new type of device, combining 2D materials with ferroelectrics, has been fabricated. Many novel devices have been fabricated, such as low power consumption memory devices, highly sensitive photo-transistors, etc. using this technique of hybrid systems incorporating ferroelectrics and 2D materials. This paper reviews two types of devices based on field effect transistor (FET) structures with ferroelectric gate dielectric construction (termed FeFET). One type of device is for logic applications, such as a graphene and TMDC FeFET for fabricating memory units. Another device is for optoelectric applications, such as high performance phototransistors using a graphene p-n junction. Finally, we discuss the prospects for future applications of 2D material FeFET.

Keywords: two-dimensional materials, ferroelectrics, FeFET, PVDF, photodetector

PACS: 71.20.Rv, 72.80.Ga, 77.55.fp, 81.05.ue **DOI:** 10.1088/1674-1056/26/3/037106

1. Introduction

The field-effect transistor (FET) is a transistor that uses an electric field to control the shape and hence the electrical conductivity of a channel of one type of charge carrier in a semiconductor material.[1] The FET structure is the basic unit for many complicated integrated, functional electrical and optoelectronic devices, such as central processor units (CPU), graphic processor units (GPU), memory and image sensors, phototransistors, photodetectors, and so on. With the end of Moore's law, the new trends of the next generation of microelectronic components need to satisfy the requirements of faster, lower power consumption, smaller size and more functionally complicated devices.[2] Under these circumstances, novel materials and new concept transistors should be urgently developed. In 2004, for the first time, Geim and Kim reported a new two-dimensional (2D) material, graphene, thus opening the gate for other 2D materials.[3,4]

During the past ten years, 2D materials have received much attention for their potential applications in future nanoelectronics and nano-optoelectronics.[5–11] These materials include graphene and 2D transition metal dichalcogenides (TMDCs), such as MoS_2, WS_2, $MoSe_2$, WSe_2, etc.[12–19] Graphene is the most famous 2D materials, and has a hexagonal lattice structure (Fig. 1(a)). The electronic band structure of graphene is totally different from that of traditional semiconductors (Fig. 1(b)).[3] As we can see, graphene is a zero bandgap material, with degenerate conduction and valance bands at the six corners of the Brillion zone.[20,21] Additionally, near the zone corners, the dispersion relation is linear rather than quadratic which resembles ultra-relativistic particles and can be described by the massless Dirac equation.[20] Therefore, the electrons in graphene are named as massless Dirac fermions, the zone corners are named as Dirac points. Another characterization of graphene is that the zero density of states at the Dirac points. So graphene behaves as a typical semimetal with a tunable Fermi level. The unique band structure of graphene has led to many intriguing phenomena, e.g., the half-integer quantum Hall effect.[4,22,23] Unlike graphene, the 2D TMDC materials are typical semiconductors. For example, most typical TMDCs, Molybdenum disulfide (MoS_2), consisting of layered S–Mo–S units structures bonded by van der Waals forces (see Fig. 1(c)), have also been widely studied in recent years.[24,25] MoS_2 is a typical semiconductor with a bandgap range from 1.2 eV to 1.8 eV as the thickness decreases from bulk to monolayer (see Fig. 1(d)).[24–26] Field effect transistors based on monolayer or multilayer MoS_2 possess high current ON/OFF ratios up to 10^7–10^8.[12,27]

*Project supported by the Major State Basic Research Development Program of China (Grant Nos. 2013CB922302 and 2016YFA0203900), the Natural Science Foundation of China (Grant Nos. 11322441, 614404147, 61574152, and 61674157), and the Key Research Project of Frontier Science of Chinese Academy of Sciences (Grant Nos. QYZDB-SSW-JSC016 and QYZDB-SSW-JSC031).

†Corresponding author. E-mail: jlwang@mail.sitp.ac.cn

‡Corresponding author. E-mail: wdhu@mail.sitp.ac.cn

© 2017 Chinese Physical Society and IOP Publishing Ltd

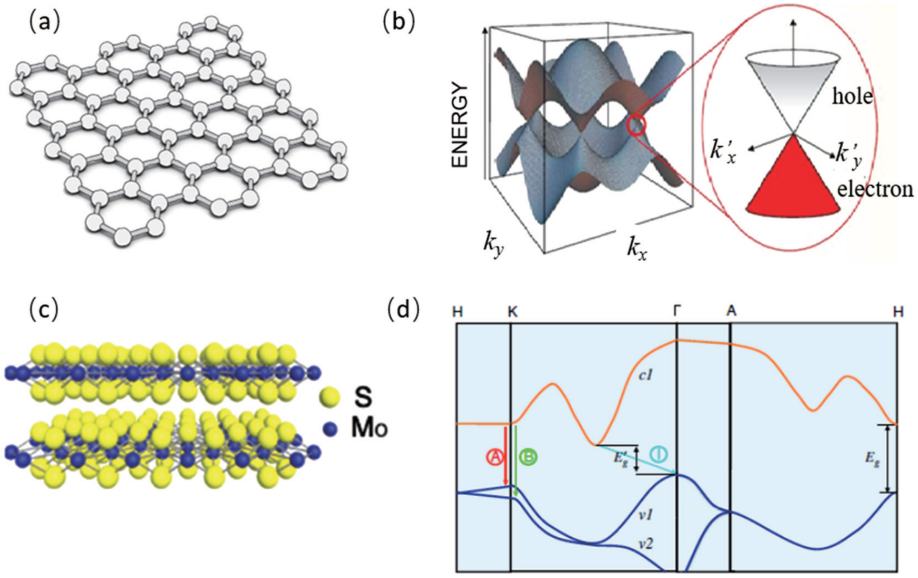


Fig. 1. (color online) (a) Schematic atomic structure of graphene. (b) Graphene band structure. Enlargement of the band structure close to the K and K', points showing the Dirac cones.[20] (c) Schematic atomic three-dimensional (3D) structure of MoS_2. (d) Simplified band structure of bulkMoS_2, showing the lowest conduction band c1 and the highest split valence bands v1 and v2. A and B are the direct-gap transitions, and I is the indirect-gap transition. E_{0g} is the indirect gap for the bulk, and E_g is the direct gap for the monolayer.[24]

Whenever we mention the transistor, the structure includes source, drain, channel, gate, and oxide gate dielectrics. As mentioned above, when we changed the traditional semiconductor to incorporate 2D material, ultra-thin channel FETs are achieved. Can other parts of the FETs be changed? Of course, we can change oxide gate dielectrics into high-k materials or other peculiar dielectrics. For instance, the dielectrics can be ferroelectrics. Ferroelectricity is a property of certain materials that have a spontaneous electric polarization that can be reversed by the application of an external electric field. The term is used in analogy to ferromagnetism, in which a material exhibits a permanent magnetic moment. The ferroelectric materials demonstrate a spontaneous nonzero polarization (after entrainment, see Fig. 2(a)) even when the applied field E is zero.[28,29] The distinguishing feature of ferroelectrics is that the spontaneous polarization can be reversed by a suitably strong applied electric field in the opposite direction; the polarization is therefore dependent not only on the current electric field but also on its history, yielding a hysteresis loop. There are many types of ferroelectrics, such as displacive type, order–disorder type, ferroelectric liquid crystals, and ferroelectric polymers.[30–35] In particular, barium titanate and lead zirconate titanate (PZT), belonging to the displacive type ferroelectrics, with a perovskite structure (see Fig. 2(b)), have been studied widely and used for different applications.[29] In recent years, ferroelectric polymers also have been studied widely and combined with many novel applications, such as polyvinylidene fluoride (PVDF) and its copolymer with polytrifluoroethylene (P(VDF-TFE)).[30–37] The structure of PVDF is a carbon chain with hydrogen and fluorine atoms. For the ferroelectric phase PVDF, the two different atoms are located on two sides of the carbon chain (called all-trans chain), as shown in Fig. 2(c).[38]

The review is organized as follows. In Section 2, the integration of ferroelectrics and 2D materials are discussed. The FeFET originated from the traditional transistor is introduced. Then, two types of devices based on the FeFET are reviewed. One type is for a memory application and another type of device is a photodetector. In Section 3, the prospects for future developments in 2D material transistors are discussed.

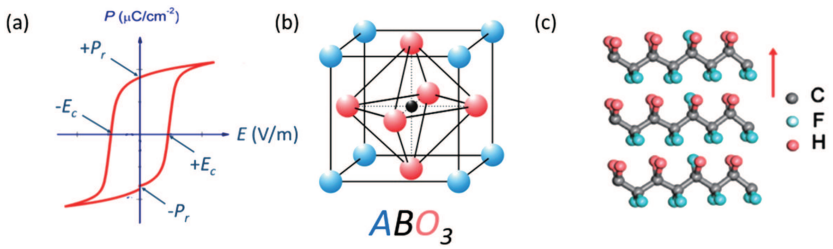


Fig. 2. (color online) (a) Typical ferroelectric hysteresis curve. P_r is the remnant polarization, and E_c is the coercive electric field. (b) Perovskite structure, similar to many ferroelectrics derived from the $BaTiO_3$ or $PbTiO_3$, is belonging to ABO_3 structure. (c) Ferroelectric PVDF structure with all-trans chain.

2. Integration of ferroelectrics and 2D materials

As mentioned in the first section, FETs have been widely used in many modern electronics applications.[39,40] As shown in Fig. 3(a), the basic structure of the FETs include source, drain, and gate terminals. If we change the channel into 2D materials and change the gate dielectrics into ferroelectrics, we obtain 2D FeFETs, as shown in Fig. 3(b). The difference between the FETs and FeFETs is the ferroelectric polarization of the gate dielectrics. The on/off characteristic can be controlled by the electrical field derived from the stable polarization.[41] In this sense, the polarization of a ferroelectric film can be stable without any bias. The first FeFETs were proposed in 1963.[42–45] Up to now, most studies on FeFETs are mainly focused on the applications for memory devices.[41,43–45] With the rapid development of 2D materials, the FeFET with a 2D material channel has been widely studied. Recently, Wang *et al.*, for the first time, reported a ferroelectric enhanced optoelectric device.[46]

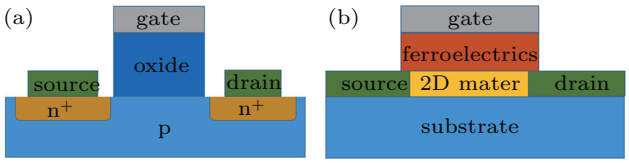


Fig. 3. (color online) (a) FET structure with traditional p-type semiconductor channel. (b) FeFET structure with 2D material channel and ferroelectric gate dielectrics.

2.1. Electronic devices incorporating 2D materials as FeFET

When we mentioned electric devices, memory is a typical one for its wide application in the modern electronics. In recent years, resistive switching type memory have been studied a lot and made a great progress.[47–49] The electronic properties of graphene have been widely studied and many unique properties have been found.[20,21,50–53] In 2009, few-layer graphene (FLG) FETs were fabricated with single-crystal epitaxial PZT films as the gate oxide, and the mobility of FLG was as high as 7×10^4.[54] Soon afterwards, Zheng *et al.* reported the development of graphene field-effect transistors with PVDF

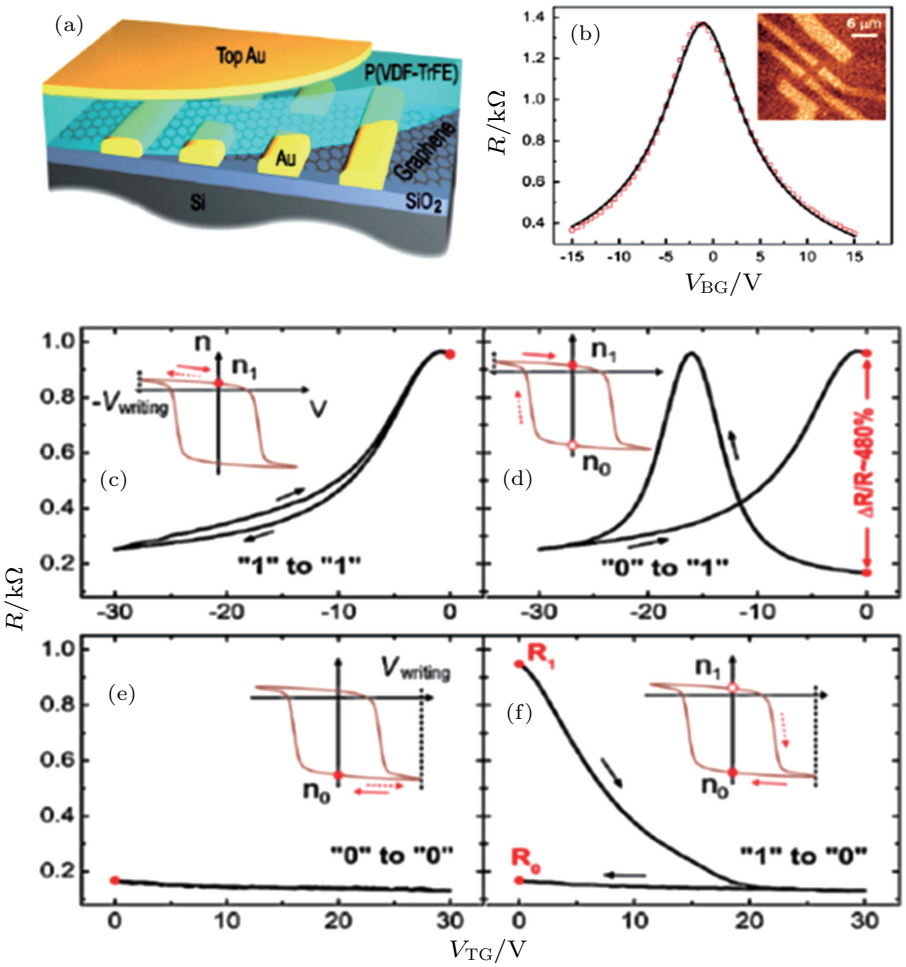


Fig. 4. (color online) (a) Sample geometry of GFeFETs.[55] (b) R vs V_{BG} of one sample after PVDF coating. The red open square and black solid lines are the experimental and fitting results, respectively. Inset: atomic force microscopy of the sample after PVDF. Color scale: 0–164 nm. (c), (d) Writing 1 by using $-V_{writing}$.[55] (e), (f) Writing 0 by using $V_{writing}$. Dashed and solid arrows indicate the forward and backward voltage sweep directions, respectively.[55]

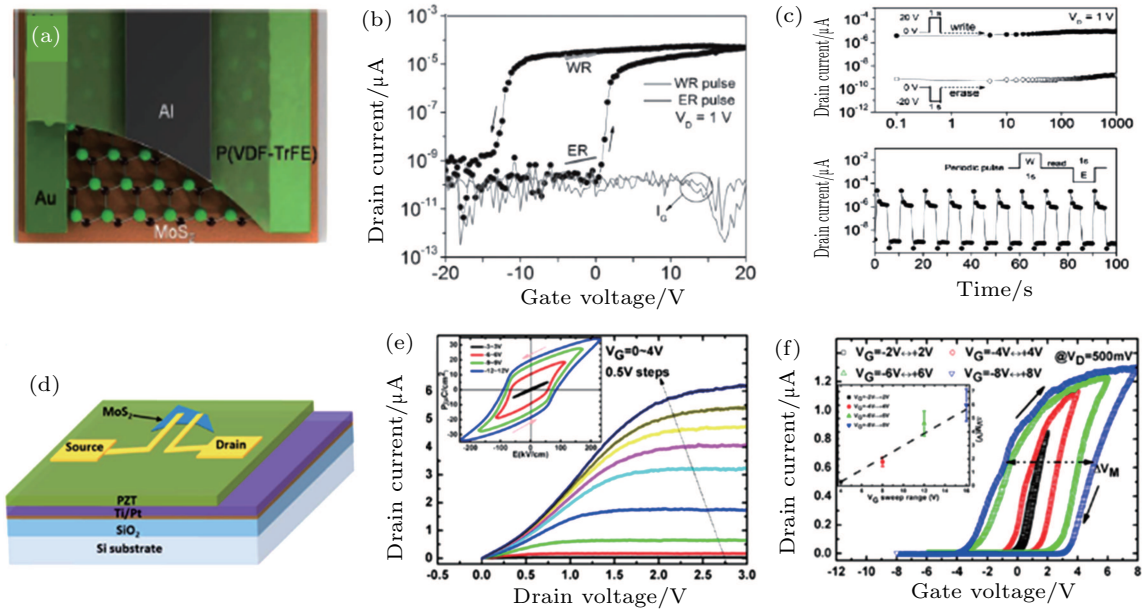


Fig. 5. (color online) (a) Schematic 3D top-view of the memory FET with the single-layer MoS_2 nanosheet of hexagonal structure, 200-nm-thick ferroelectric P(VDF-TrFE) polymer, and Al gate.[56] (b) The transfer curve of top-gate-driving single-layer MoS_2 transistor with P(VDF-TrFE) ferroelectric layer; V_G sweep range is from -20 to $+20$ V and $V_D = 1$ V. Memory hysteresis window of the transistor with 200-nm-thick P(VDF-TrFE) polymer appears to be ~ 14 V. Short pulses of $+20$ and -20 V on the gate lead to two distinct states of WR and ER, respectively, as shown overlapped with the memory hysteresis curve. I_G from the P(VDF-TrFE) polymer was below ~ 100 pA.[56] (c) The figure above is the retention properties of WR and ER states recorded under $V_D = 1$ V and $V_G = 0$ V for 1000 s. Inset shows the ± 20 V 1 s pulse for retention measurements. The following figure is the current dynamics of our memory transistor in response to repetitive input voltage pulses under $V_D = 1$ V. The inset figure shows the periodic pulse mode for WR/read/ER/read process.[56] (d) Schematics of MoS_2-PZT FETs device.[57] (e) Output characteristics of MoS_2-PZT device. Gate voltage is applied from 0 V to 4 V with a 0.5 V step. Drain voltage is swept from 0 V to 3 V. The inset is *P*–*E* curves of a 260-nm-thick PZT under different voltages ranging from -3 to $+3$ V up to -12 to $+12$ V at 100 Hz.[57] (f) The transfer curves of MoS_2-PZT FET at $V_D = 500$ mV. Memory window variation with increasing V_G sweep range is shown in the inset.[57]

ferroelectric gating.[55] The sample geometry structure is shown in Fig. 4(a). The resistance versus gate voltage characteristics (R vs V_{BG}) are shown in Fig. 4(b), where the Hall mobility is approximately 4600 $cm^2 \cdot V^1 \cdot s^1$ and the gate dielectric is SiO_2. Based on this type of device structure and electrostatic effect, bit writing in graphene FeFETs can be significantly simplified by switching the ferroelectric polarization between P_r and P_r, using symmetrical voltage sweeps. With $n_{BG} = -\beta P_r/e$, to write the high resistance "1," a negative writing voltage ($V_{writing}$) is applied to the ferroelectric, setting the dipole polarization to P_r independent of the initial states in the unit cell (Figs. 4(c) and 4(d)). In contrast, a positive $V_{writing}$ with the same magnitude sets the FeFET into low resistance "0" (Figs. 4(e) and 4(f)). This work shows the possibility that the graphene FeFET can be used as non-volatile memory. Similar results based on different ferroelectric films have been reported in other research groups.[23,55] It is well known that graphene is a zero bandgap 2D material, and the on/off ratio of a graphene-based transistor is relatively small. MoS_2 is a typical 2D semiconductor with a bandgap of 1.2–1.8 eV. 2D MoS_2 transistors have been prepared by the same exfoliation technique, and the on/off ratio is up to 6 to 8 orders. In 2012, Im *et al.* achieved a 2D MoS_2 FeFET with single to triple-layered MoS_2 nano-sheets adopting a ferroelectric polymer P(VDF-TrFE).[56] The schematic 3D top-view of the memory FET with the single-layer MoS_2 nano-sheet of hexagonal structure, 200-nm-thick ferroelectric P(VDF-TrFE) polymer, and Al gate is shown in Fig. 5(a). The device shows the high on/off I_D ratio of 10^5, and good retention properties in both static and dynamic switching, maintaining a high program/erase ratio of $\sim 5 \times 10^3$, as shown in Figs. 5(b) and 5(c). Recently, Zhu *et al.* prepared MoS_2 field-effect transistors with a PZT ferroelectric gating structure.[57] The structure of the device is shown in Fig. 5(d) and the ferroelectric related electrical properties are shown in Figs. 5(e) and 5(f), respectively. Additionally, many novel applications based on graphene and other 2D materials with FeFET structure have been put forward recently.[58–61] These devices open a new path for next generation electronics.

2.2. Optoelectric devices of 2D materials on FeFET

There are many studies on the optoelectric properties of graphene and other 2D semiconductors, such as light-emitting devices and photodetectors.[12,14,15,56] In this section, we mainly focus on the photodetecting properties of the 2D materials. The studies of 2D photodetectors are increasing rapidly. Most of these 2D material photodetectors are based on the transistor structure. Graphene photodetectors have been widely studied, and the sensitive wavelength range covers visible to long-wavelength infrared wavelengths, and even to terahertz frequencies.[52,53,62] However, the responsivity and detectivity of these graphene photodetectors is relatively low

compared with that of traditional photodetectors. With the emergence of 2D TMDCs, phototransistors with high responsivity have been achieved.[63–65] As is known, for practical applications, dark current is one of the most important factors. For the traditional device, to suppress dark current, a stable gate voltage is needed to be continuously applied. These are not significant negative factors for real applications of the device. Recently, Wang *et al.* presented a new type of 2D photodetector based on the FeFET structure.[46] The structure of the device is shown in Fig. 6(a). The transfer curves $I_{sd} - V_{tg}$ (drain-source current I_{sd} as a function of top gate voltage V_{tg}) of the MoS_2 transistor with ferroelectric polymer were investigated at room temperature (shown in Fig. 6(b)). The $V_{sd} - I_{sd}$ characteristics (without additional gate voltage) of these three states are shown in Fig. 6(c). In P_{up} state, I_{sd} is the lowest compared to that of the other two states. This situation means that the depleted state of carriers in the MoS_2 channel is caused by the electrostatic field derived from the remnant polarization of P(VDF-TrFE). The cross section of the device structure and the equilibrium energy band diagram of this state are shown in Fig. 6(d). While in the P_{up} state, the generated photo current dominates the channel current, resulting in a highly-efficient photocurrent extraction and increased photoresponse, as shown in Fig. 6(e). The most interesting point is that the electric field from the remnant polarization can tune the bandgap of 2D MoS_2. Based on this structure and the large electric field effect, response wavelength of the 2D MoS_2 photodetector have been broadened from 0.85 to 1.55 μm, as shown in Fig. 6(f). Compared with traditional infrared photodetector, this type of device opens a new method to prepare infrared photodetectors.[66,67] Subsequently, several photodetectors have been achieved employing the 2D FeFET structure.[68,69] In addition to the TMDCs FeFET photodetector, the p-n junction device has been proposed by the Martin group.[70] They transferred graphene onto single domain $LiNbO_3$ substrates. Raman spectroscopy of graphene for a G-band frequency map and Graphene G-peak have been achieved on the different polarization states (up and down polarized), as shown in Figs. 7(a) and 7(b). Additionally, the gate-dependent Raman spectroscopy of graphene unipolar and periodically poled $LiNbO_3$ is also tested (see Figs. 7(c) and 7(d)). These results indicate that different polarization states dope graphene in different types. It is a new way to form a p–n junction. Indeed, the p–n junction at the domain wall results in the maximum photocurrent, as shown in Fig. 7(e). Such an approach is not only suitable for 2D materials, but is also suitable for one-dimensional nanowires. For instance, our group has obtained high performance nanowire photodetectors in this way.[71,72] Therefore, utilizing the polarization of ferroelectrics to act on 2D materials may open a new approach for 2D materials application in optoelectronics.

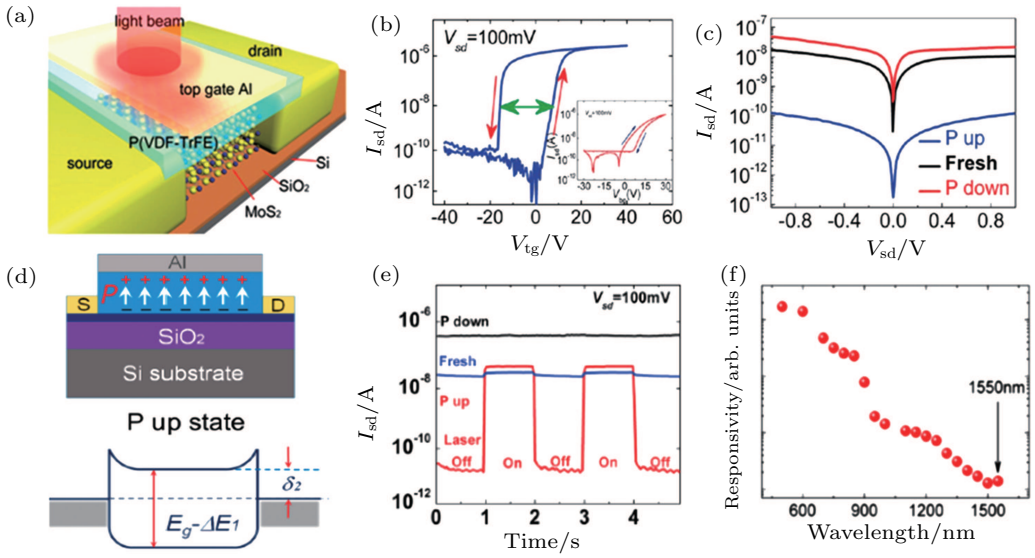


Fig. 6. (color online) (a) 3D schematic view of the triple-layer MoS_2 photodetector with monochromatic light beam.[46] (b) The transfer curves of triple-layer MoS_2 channel with P(VDF-TrFE) ferroelectric polymer gate on dark state at room temperature. The transfer characteristics of triple-layer MoS_2 with SiO_2 back-gate are shown in the inset.[46] (c) $V_{sd} - I_{sd}$ characteristics (at ZERO gate voltage) with three ferroelectric polarization states in the ferroelectric layer. The three states are: fresh state (ferroelectric layer without polarization), polarization up ("P_{up}" polarized by a pulse V_g of −40 V), and polarization down ("P_{down}" polarized by a pulse V_g of −40 V) states, respectively.[46] (d) The cross section structures of the device and equilibrium energy band diagrams of ferroelectric polarization up state with $V_{sd} = 0$ V. E_g is the bandgap of MoS_2. δ_2 is the height from bottom of conduction band to the Fermi level.[46] (e) Photo switching behavior of ferroelectric polarization gating triple-layer MoS_2 photodetector at three states ($\lambda = 635$ nm, $V_{sd} = 100$ mV, and $P = 100$ nW).[46] (f) Responsitivity of similar polarization-gating triple layer MoS_2 photodetector as a function of light wavelength from 500 nm to 1550 nm at $V_{sd} = 1$ V, $P = 100$ mW under P_{up} state.[46]

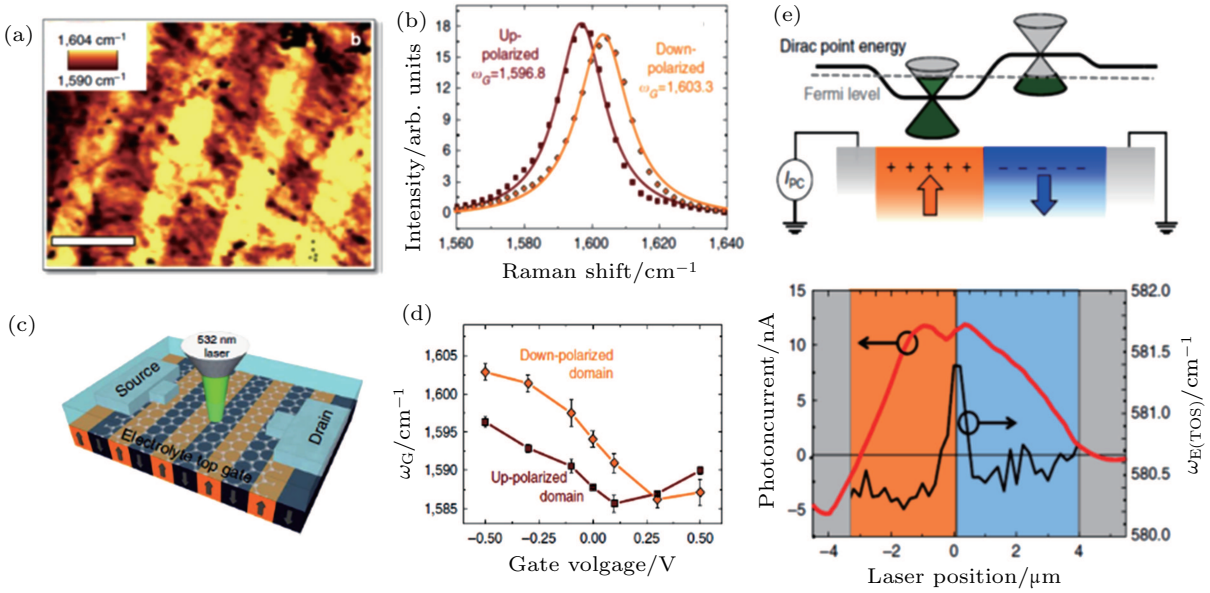


Fig. 7. (color online) (a) Graphene G-band frequency map. Scale bars, 10 μm.[70] (b) Graphene G-peak averaged over a dark and a bright stripe in panel (a) with the G-band frequency $\omega = 1603.3$ cm^{-1} and 1596.8 cm^{-1} for bright and dark stripes, respectively. Lines correspond to Lorentzian fits to the experimental data (orange diamonds for the bright stripe and dark-red squares for the dark stripe).[70] (c) Schematic of a top-gated graphene transistor on periodically poled $LiNbO_3$.[70] (d) Representative gate-dependent Raman G-band frequency averaged over a down-polarized domain (orange diamonds) and an up-polarized domain (dark-red squares). Error bars indicate the s. d. of the frequency within each stripe.[70] (e) Photocurrent response of a ferroelectricity-induced p–n junction in graphene. The red line represents the photocurrent response of a top-gated graphene transistor with a gate voltage of 400 mV on periodically poled $LiNbO_3$. The simultaneously detected Raman E(TO8) frequency (black) along the same line was used to identify the down polarized (blue) and up-polarized (orange) domains of the $LiNbO_3$. Grey shading corresponds to the Ti/Pd contacts. A schematic band diagram can be constructed based on the experimental observations.[70]

3. Conclusion and outlook

Ferroelectric materials have been studied for many years and their related devices have been widely used. 2D materials, beginning with graphene, have drawn much attention for only the past ten years. Here we reviewed recent progress on ferroelectric enhanced 2D material devices, in which ferroelectric materials and 2D materials are combined together. We believe that integrating 2D materials with ferroelectrics to form the FeFET maybe a possible way for unique applications in memory devices and photodetectors. In other words, the FeFET could represent a new direction for developing advanced capabilities required for next-generation nano-electronic and optoelectronic devices.

References

[1] Millman J 1985 *Electronic Devices and Circuits* (Singapore: McGraw-Hill International) p. 397
[2] Waldrop M M 2016 *Nature* **530** 7589
[3] Novoselov K S, Geim A K, Morozov S V, Jiang D, Zhang Y, Dubonos S V and Grigorieva I V 2004 *Science* **306** 5696
[4] Novoselov K S, Geim A K, Morozov S V, Jiang D, Katsnelson M I, Grigorieva I V, Dubonos S V and Firsov A A 2005 *Nature* **438** 7065
[5] Wang Q H, Kalantar-Zadeh K, Kis A, Coleman J N and Strano M S 2012 *Nature Nanotechnology* **7** 699
[6] He Q Y, Zeng Z Y, Yin Z Y, Li H, Wu S X, Huang X and Zhang H 2012 *Small* **8** 2994
[7] Pu J, Yomogida Y, Liu K K, Li L J, Iwasa Y and Takenobu T 2012 *Nano Lett.* **12** 4013
[8] Britnell L, Gorbachev R V, Jalil R, Belle B D, Schedin F, Mishchenko A, Georgiou T, Katsnelson M I, Eaves L, Morozov S V, Peres N M R, Leist J, Geim A K, Novoselov K S and Ponomarenko L A 2012 *Science* **335** 947
[9] Avouris P, Freitag M and Perebeinos V 2008 *Nat. Photon.* **2** 341
[10] Scholes G D and Rumbles G 2006 *Nat. Mater.* **5** 683
[11] Kamat P V 2008 *J. Phys. Chem. C* **112** 18737
[12] Lopez-Sanchez O, Lembke D, Kayci M, Radenovic A and Kis A 2013 *Nature Nanotechnology* **8** 497
[13] Roy K, Padmanabhan M, Goswami S, Sai T P, Ramalingam G, Raghavan S and Ghosh A 2013 *Nature Nanotechnology* **8** 826
[14] Zhang W, Chuu C P, Huang J K, Chen C H, Tsai M L, Chang Y H, Liang C T, Chen Y Z, He J H, Chou M Y and Li L J 2014 *Sci. Rep.* **4** 3826
[15] Zhang W, Huang J K, Chen C H, Chang Y H, Cheng Y J and Li L J 2013 *Adv. Mater.* **25** 3456
[16] Georgiou T, Jalil R, Belle B D, Britnell L, Gorbachev R V, Morozov S V, Kim Y J, Gholinia A, Haigh S J, Makarovsky O, Eaves L, Ponomarenko L A, Geim A K, Novoselov K S and Mishchenko A 2013 *Nature Nanotechnology* **8** 100
[17] Abderrahmane A, Ko P J, Thu T V, Ishizawa S, Takamura T and Sandhu A 2014 *Nanotechnology* **25** 365202
[18] Xia J, Huang X, Liu L Z, Wang M, Wang L, Huang B, Zhu D D, Li J J, Gu C Z and Meng X M 2014 *Nanoscale* **6** 8949
[19] Britnell L, Ribeiro RM, Eckmann A, Jalil R, Belle BD, Mishchenko A, Kim Y J, Georgiou T, Morozov S V, Grigorenko A N, Geim A K, Casiraghi C, Castro Neto A H and Novoselov K S 2013 *Science* **340** 1311
[20] Castro Neto A H, Guinea F, Peres N M R, Novoselov K S and Geim A K 2009 *Rev. Mod. Phys.* **81** 109
[21] Das Sarma S, Adam S, Hwang E H and Rossi E 2011 *Rev. Mod. Phys.* **83** 407
[22] Zhang Y, Tan Y W, Stormer H L and Kim P 2005 *Nature* **438** 201
[23] Wang X R, Shi Y and Zhang R 2013 *Chin. Phys. B* **22** 098505
[24] Mak KF, Lee C, Hone J, Shan J and Heinz T F 2010 *Phys. Rev. Lett.* **105** 136805
[25] Novoselov K S, Jiang D, Schedin F, Booth T J, Khotkevich V V, Morozov S V and Geim A K 2005 *Proceedings of the National Academy of Sciences of the United States of America* **102** 10451
[26] Lee C, Yan H, Brus L E, Heinz T F, Hone J and Ryu S 2010 *ACS Nano* **4** 2695
[27] Bertolazzi S, Krasnozhon D and Kis A 2013 *ACS Nano* **7** 3246
[28] Valasek J 1921 *Phys. Rev.* **17** 475
[29] Dawber M, Rabe K M and Scott J F 2005 *Rev. Mod. Phys.* **77** 1083

[30] Yuan S Z, Meng X J, Sun J L, Cui Y F, Wang J L, Tian L and Chu J H 2011 *Phys. Lett. A* **375** 1612

[31] Wang J L, Yuan S Z, Tian L, Meng X J, Sun J L and Chu J H 2011 *Appl. Phys. Lett.* **98** 052906

[32] Tian B B, Chen Z H, Jiang A Q, Zhao X L, Liu B L, Wang J L, Han L, Sun S, Sun J L, Meng X J and Chu J H 2013 *Appl. Phys. Lett.* **103** 042909

[33] Wang J L, Liu B L, Zhao X L, Tian B B, Zou Y H, Sun S, Shen H, Sun J L, Meng X J and Chu J H 2014 *Appl. Phys. Lett.* **104** 182907

[34] Zhao X L, Tian B B, Liu B L, Wang J L, Han L, Sun J L, Meng X J and Chu J H 2014 *Thin Solid Films* **551** 171

[35] Zhao X L, Wang J L, Liu B L, Tian B B, Zou Y H, Sun S, Sun J L, Meng X J and Chu J H 2014 *Appl. Phys. Lett.* **104** 082903

[36] Zhang Q M, Bharti V and Zhao X 1998 *Science* **280** 2101

[37] Chu B J, Zhou X, Ren K L, Neese B, Lin M R, Wang Q, Bauer F and Zhang Q M 2006 *Science* **313** 334

[38] Ducharme S, Bune A V, Fridkin V M, Blinov L M, Palto S P, Sorokin A V, Yudin S G and Zlatkin A 1998 *Nature* **391** 874

[39] Norbert R and Malik 1995 Electronic Circuits: Analysis, Simulation, and Design (NJ: Prentice Hall) pp. 315–316

[40] Ghausi M S 2001 *Microelectronic Circuits* (NJ: Pearson Education/Prentice-Hall) p. 102

[41] Naber R C G, Tanase C, Blom P W M, Gelinck G H, Marsman A W, Touwslager F J, Setayesh S and De Leeuw D W 2005 *Nat. Mater.* **4** 243

[42] Sugibuchi K, Kurogi Y and Endo N 1975 *J. Appl. Phys.* **46** 2877

[43] Miller S L and McWhorter P J 1992 *J. Appl. Phys.* **72** 5999

[44] Aziz A, Ghosh S, Datta S and Gupta S K 2016 *IEEE Electron Dev. Lett.* **37** 805

[45] Perlman S S and Ludewig K H 1967 *IEEE Transactions on Electron Devices* **ED14** 816

[46] Wang X D, Wang P, Wang J L, Hu W, Zhou X, Guo N, Huang H, Sun S, Shen H, Lin T, Tang M H, Liao L, Jiang A Q, Sun J L, Meng X J, Chen X S, Lu W and Chu J H 2015 *Adv Mater.* **27** 6575

[47] Lu N, Sun P X, Li L, Liu Q, Long S B, Lv H B and Liu M 2016 *Chin. Phy. B* **25** 056501

[48] Dai Y H, Pan Z Y, Chen Z, Wang F F, Li N, Jin B and Li X F 2016 *Acta Phys. Sin.* **65** 073101 (in Chinese)

[49] Liu S, Lu N D, Zhao X L, Xu H, Banerjee W, Lv H B, Long S B, Qing J, Liu Q and Liu M 2016 *Adv. Mater.* (Deerfield Beach, Fla)

[50] Geim A K and Novoselov K S 2007 *Nat. Mater.* **6** 183

[51] Geim A K 2009 *Science* **324** 1530

[52] Mueller T, Xia F and Avouris P 2010 *Nat. Photon.* **4** 297

[53] Xia F, Mueller T, Lin Y M, Valdes-Garcia A and Avouris P 2009 *Nat. Nanotech.* **4** 839

[54] Hong X, Posadas A, Zou K, Ahn C H and Zhu J 2009 *Phys. Rev. Lett.* **102** 136808

[55] Zheng Y, Ni G X, Toh C T, Tan C Y, Yao K and Ozyilmaz B 2010 *Phys. Rev. Lett.* **105** 166602

[56] Lee H S, Min S W, Park M K, Lee Y T, Jeon P J, Kim J H, Ryu S and Im S 2012 *Small* **8** 3111

[57] Zhang X W, Xie D, Xu J L, Sun Y L, Li X, Zhang C, Dai R X, Zhao Y F, Li X M, Li X and Zhu H W 2015 *IEEE Electron Dev. Lett.* **36** 784

[58] Song E B, Lian B and Min Kim S 2011 *Appl. Phys. Lett.* **99** 042109

[59] Raghavan S, Stolichnov I, Setter N, Heron J S, Tosun M and Kis A 2012 *Appl. Phys. Lett.* **100** 023507

[60] Yusuf M H, Nielsen B, Dawber M and Du X 2014 *Nano Lett.* **14** 5437

[61] Doh Y J and Yi G C 2010 *Nanotechnology* **21** 105204

[62] Bonaccorso F, Sun Z, Hasan T and Ferrari A C 2010 *Nat. Photon.* **4** 611

[63] Lopez-Sanchez O, Lembke D, Kayci M, Radenovic A and Kis A 2013 *Nat. Nanotech.* **8** 497

[64] Yin Z Y, Li H, Li H, Jiang L, Shi Y M, Sun Y H, Lu G, Zhang Q, Chen X D and Zhang H 2012 *ACS Nano* **6** 74

[65] Lee H S, Min S W, Chang Y G, Park M K, Nam T, Kim H, Ryu S and Im S 2012 *Nano Lett.* **12** 3695

[66] Qiu W C and Hu W D 2015 *Science China-Physics Mechanics & Astronomy* **58** 027001

[67] Hu W D, Liang J, Yue F Y, Chen X S and Lu W 2016 *Journal of Infrared and Millimeter Waves* **35** 25

[68] Huang H, Wang X D and Wang P 2016 *RSC Adv.* **6** 87416

[69] Wu G J, Wang X D, Wang P, Huang H, Chen Y, Sun S, Shen H, Lin T, Wang J L, Tian B B, Sun J L, Meng X J and Chu J H 2016 *Nanotechnology* **27** 364002

[70] Baeumer C, Saldana-Greco D, Martirez J M P, Rappe A M, Shim M and Martin L W 2015 *Nat Commun.* **6** 6136

[71] Zheng D S, Wang J L, Hu W D, Liao L, Fang H H, Guo N, Wang P, Gong F, Wang X D, Fan Z Y, Wu X, Meng X J, Chen X S and Lu W 2016 *Nano Lett.* **16** 2548

[72] Zheng D S, Fang H H, Wang P, Luo W J, Gong F, Ho J C, Chen X S, Lu W, Liao L, Wang J L and Hu W D 2016 *Adv. Function. Mater.* **26** 7690

[73] Chen Y, Wang X D, Wang P, Huang H, Wu G J, Tian B B, Hong Z C, Wang Y T, Sun S, Shen H, Wang J L, Hu W D, Sun J L, Meng X J, Chu J H 2016 *ACS Applied Materials & Interfaces.* **8** 32083

[74] Fang H H and Hu W D 2017 *Science China-Physics Mechanics & Astronomy.* **60** 027031